Check for updates

Two physical processes enhanced the performance of *Auricularia auricula* dreg in Cd(II) adsorption: composting and pyrolysis

Yue Li, Siqi Huang, Yingnan Wei, Xuesheng Liu, Meng Zhang, Zonghui Jin, Hongmei Wang and Juanjuan Qu

ABSTRACT

This study aims to discover the impact of composting and pyrolysis on the adsorption performance of *Auricularia auricula* dreg (AAD) for Cd(II) in aqueous solution. *Auricularia auricula* dreg (AAD), *Auricularia auricula* dreg biochar (AADB) and *Auricularia auricula* dreg compost (AADC) were used to remove Cd(II) from aqueous solution, and their adsorption conditions and mechanisms were compared. The adsorption quantity of three adsorbents reached the maximum (AAD: 80.0 mg/g, AADB: 91.7 mg/g, AADC: 93.5 mg/g) under same conditions (adsorbent dosage of 1 g/L, pH 5.0, biosorption temperature of 25 °C, and biosorption time of 120 min). All Cd(II) biosorption processes onto three adsorbents complied with the Langmuir isotherm model and the pseudo-second-order kinetic equation, and spontaneously occurred in an order of AADC > AADB > AAD. The difference in biosorption quantity relied on variation in surface structure, crystal species and element content caused by composting or pyrolysis. Composting enhanced the changes in surface structure, crystal species, functional groups and ion exchange capacity of the AAD, resulting in AAD had greatly improved the biosorption quantity of Cd(II). Pyrolysis increased the adsorption of Cd(II) mainly by increasing the Brunauer–Emmett–Teller (BET) surface area, the particle size and pH, in the same time, providing more oxygen-containing functional groups.

Key words | *Auricularia auricula* dreg, biochar, biosorption mechanism, Cd(II), compost

Yue Li
Siqi Huang
Yingnan Wei
Xuesheng Liu
Meng Zhang
Zonghui Jin
Juanjuan Qu (corresponding author)
College of Resources and Environmental Science,
Northeast Agricultural University,
Harbin 150030,
China
E-mail: *juanjuan4050234@163.com*

Hongmei Wang
College of Life Sciences,
Shandong Normal University,
Jinan 250014,
China

INTRODUCTION

Cadmium, as one of the most toxic heavy metals causing abdominal pain, nausea, muscle cramps, bone marrow damage, and kidney stones (Lee *et al.* 2012), has been classified as class I carcinogen by the international cancer institute. Cadmium-containing industrial wastewater has seriously threatened human health and caused ecological damage. China's environmental protection law stipulates that the maximum allowable emission concentration of cadmium in industrial wastewater is 1.0 mg/L and the maximum allowable emission concentration of cadmium is 0.1 mg/L. The traditional methods including chemical precipitation, electrolysis, biosorption, membrane separation and ion exchange have been employed to treat the industrial wastewater (Bayo 2012), among which biosorption method has more advantages in cost, operation process and high efficiency for low concentration metal-contaminated water.

Auricularia auricula dreg (AAD) is an agricultural by-product with a wide range of sources and a relative low price in mushroom production. The main components of this waste dreg include sugars, organic acids, and biologically active substances, on which distribute hydroxyl, carboxyl, amide, and phosphate groups that can chelate heavy metal ions in wastewater. In our previous study, AAD has been used to remove lead(II) and Cr(VI) (Dong *et al.* 2017; Song *et al.* 2017a) and chemically modified AAD has been used to adsorb Cd(II) (Song *et al.* 2017b), however, its biosorption efficiency is still lower than that of other biosorbents derived from agricultural byproduct (Mukherjee *et al.* 2011). To improve the biosorption capacity, a physical process such as pyrolysis and composting is also employed to treat the adsorbents. Biochar is a highly aromatic and difficult-to-penetrate solid material resulting

doi: 10.2166/wst.2019.147

Downloaded from http://iwa.silverchair.com/wst/article-pdf/79/8/1511/617908/wst079081511.pdf
by guest

from pyrolysis under hypoxia or low oxygen. The aromatic sheets provide biochar with a loose and porous structure, moreover, a large number of oxygen-containing groups such as phenolic hydroxyl, carboxyl and carbonyl groups formed during pyrolysis are beneficial to the biosorption of metallic ions (Kumar *et al.* 2013; Regmi *et al.* 2012; Lin *et al.* 2012). Composting is an aerobic process that decomposes the organic material into humus-like material (Naja & Volesky 2006). After composting, the agricultural waste changes to a highly porous and complex mixtures with abundant functional groups and strong ion exchange capacity. During composting, organic matter is decomposed and transformed into stable humic compounds, which have the ability to combine with metal ions. In the composting process, many hydrophilic groups will be produced, which will increase the adsorption of heavy metal ions in the compost. Studies have shown that compost has a highly complex mixture of polymer functional groups and high ion exchange capacity. Moreover, the compost is also rich in lignin and chitin, which are the reasons why compost has a good adsorption effect on metal ions in high-concentration metal ion industrial wastewater (Mattuschka & Straube 1993).

This study aims to compare the biosorption for Cd(II) among the three kinds of adsorbents prepared from *Auricularia auricula* dreg. The optimal experimental conditions including pH, adsorbent dosage, biosorption temperature and biosorption time were explored in the batch experiments. The biosorption characteristics were discussed by isotherm, kinetic equation and thermodynamic analysis. The biosorption mechanisms were revealed by scanning electron microscopy (SEM), surface area analyzer, Fourier transform infrared (FTIR) spectroscopy, X-ray diffraction (XRD), X-ray photoelectron spectroscopy (XPS) and analysis in pH, zeta potential, Brunauer–Emmett–Teller (BET), cation exchange capacity (CEC) and oxygen-containing functional groups.

MATERIALS AND METHODS

Adsorbents preparation

Auricularia auricula dreg was provided by Xiangfang edible fungi plant, Harbin, China. AAD was rinsed with distilled water, dried to constant weight at 70 °C, and ground into powders less than 0.3 mm in diameter. *Auricularia auricula* dreg bichar (AADB) was obtained by heating ADD in a muff oven at 500 °C for 120 min. *Auricularia auricula* dreg compost (AADC) was prepared by mixing AAD with cow dung at ratio of 1:1 and fermenting at room temperature for 3 months, then the acquired adsorbent was dried and ground into powders in a diameter of 0.3 mm.

Chemicals and reagents

All chemicals used in this study were of analytical grade. The stock solution (1 g/L) of Cd(II) was prepared by dissolving 2.7442 g of cadmium nitrate ($Cd(NO_3)_2.4H_2O$) (Guangfu Fine Chemical, Tianjin, China) in 1 L of deionized water and work solution at desired concentration was prepared by diluting stock solution. The initial pH was adjusted with 0.1 M NaOH (Kermel Chemical Reagent Co., Ltd, Tianjin, China) or 0.1 M HCl (Pilot Chemical Co., Shanghai, China) solution.

Batch biosorption experiments

The batch biosorption experiments were conducted in 150 mL Erlenmeyer flask containing 100 mL of diluted Cd(II) solution. The experiments were operated at different conditions: pH of 2, 3, 4, and 5, adsorbent dosage of 1, 2, 3, 4, and 5 g/L, biosorption temperature of 20, 25, 30, and 35 °C, and biosorption time of 20, 40, 60, 80, 100, and 120 min. When the biosorption reached equilibrium, the samples were filtered and the residual amount of Cd(II) was determined using atomic absorption spectrophotometer (AA-6800 model, Shimadzu-GL, Japan). The biosorption quantity (Q) for Cd(II) were calculated with the following equations:

$$Q = \frac{(C_0 - C_e)v}{m} \quad (1)$$

where C_0 and C_e are the initial and the equilibrium concentration of Cd(II) in solution (mg/L), respectively; m is mass of adsorbent (g) and v is the volume of reaction solution (L).

Biosorption isotherm model

Biosorption isotherm refers to the relationship of the metal ion concentration between the liquid phase and the solid phase (adsorbent) reaching equilibrium at a certain temperature (Hu *et al.* 2011; Kwon & Jeon. 2012). In this study, Langmuir and Freundlich isotherm models were used to fit the experimental data. The biosorption isotherms were carried out at 303 K, the adsorbent dosage of 1 g/L, the rotation speed of 160 r/min, the biosorption time of 120 min, the solution pH of 5, and the initial concentration of Cd(II) varying from 25–100 mg/L. The Langmuir and Freundlich isotherm equation were expressed as follows.

Downloaded from http://iwa.silverchair.com/wst/article-pdf/79/8/1511/617908/wst079081511.pdf
by guest

Langmuir isotherm equation (Langmuir 1918):

$$Q = \frac{Q_{max} K_L C_e}{1 + K_L C_e} \quad (2)$$

Freundlich isotherm equation (Freundlich & Helle 1939):

$$\ln Q_e = \frac{1}{n} \ln C_e + \ln K_F \quad (3)$$

where Q_e is the equilibrium biosorption quantity of Cd(II) (mg/g); Q_{max} is the maximum biosorption quantity in theory (mg/g); C_e is the equilibrium concentration of Cd(II) in solution (mg/L; and K_L is the Langmuir equilibrium biosorption constant (L/mg)); K_F is the Freundlich constant associated with the biosorption quantity; n represents a constant relating to the biosorption intensity.

Biosorption kinetics

Pseudo-first-order model and pseudo-second-order model were used to describe the biosorption characteristics. The experiment was carried out at 303 K, the adsorbent dosage of 1 g/L, pH 5, and initial concentration of 100 mg/L. The concentration of Cd(II) was measured after the sample was taken at 20, 40, 60, 80, 100 and 120 min, respectively. The kinetic models were expressed as follows.

The pseudo-first-order kinetic model:

$$\lg (q_e - q_t) = \lg q_e - \frac{k_1 t}{2.303} \quad (4)$$

The pseudo-second-order kinetic model:

$$\frac{t}{q_t} = \frac{1}{k_2 q_e^2} + \frac{t}{q_e} \quad (5)$$

where q_e is the biosorption quantity of Cd(II) at equilibrium (mg/g); q_t is the biosorption quantity at time t (mg/g); t is the biosorption time (min); k_1 is the rate constant of pseudo-first-order biosorption (1/min); k_2 is the rate constant of pseudo-second-order biosorption (g/mg·min).

Biosorption thermodynamics

The thermodynamic study was carried out at 298 K. Gibbs free energy (ΔG°) was given as follows:

$$\Delta G^\circ = -RT \ln K \quad (6)$$

$$K = \frac{q_e}{c_e} \quad (7)$$

where R is the universal gas constant (8.314 J/(mol·K)); T is the absolute temperature in Kelvin (K); K is for biosorption equilibrium constant; q_e is the biosorption quantity of Cd(II) (mg/g); c_e is the equilibrium concentration of Cd(II).

Biosorption mechanism

Scanning electron microscopy (SEM) (QuANTA200 model, American FEI, USA) and energy-dispersive X-ray spectroscopy (EDX) (LEO 1455 VP/EDX Oxford 300, UK) were used to analyze the surface morphology and element content of adsorbents; Fourier transform infrared spectrometer (Alpha, Bruker, Germany) was used to analyze the functional groups; X-ray diffraction (XRD) (D/max2200 model, Hitachi, Japan) was employed to detect the crystalline structure; the element composition of adsorbent loaded with cadmium ions was analyzed by XPS (VG Scientific EACALab220i-XL). Surface area analyzer (ASAP 2020, Micromeritics, USA) was applied to determine the specific surface area, the pore volume and the pore diameter of three adsorbents; pH meter (Corning, Model 140) was used to measure the pH of the adsorbents; the potential of the fine particles (Zeta) of the sample were measured by a type of micro-electrophoresis apparatus (JS94F). Cation exchange capacity (CEC) was measured with sodium acetate-flame photometric method. Boehm titrations were used to differentiate and quantify oxygen based functional groups.

RESULTS AND DISCUSSION

Batch biosorption experiments

Effect of solution pH

The effect of solution pH has a great influence on the biosorption process of heavy metal ions. In this study, the solution pH between 2 and 5 was set to prevent the formation of cadmium precipitates (Chen & Chen 2009). The effect of solution pH on Cd(II) biosorption onto the three kinds of adsorbents is shown in Figure 1(a). At pH 2 to 5, the biosorption quantity of the three adsorbents obviously increased with the increased pH value and reached maximum of 80.0, 91.7 and 93.5 mg/g for AAD, AADB and AADC at pH 5, respectively. Apparently, at all tested pH, the biosorption quantity of AADC and AADB were higher than that of AAD, and the maximum biosorption quantities of AADC and AABD were higher than that

Downloaded from http://iwa.silverchair.com/wst/article-pdf/79/8/1511/617908/wst079081511.pdf
by guest

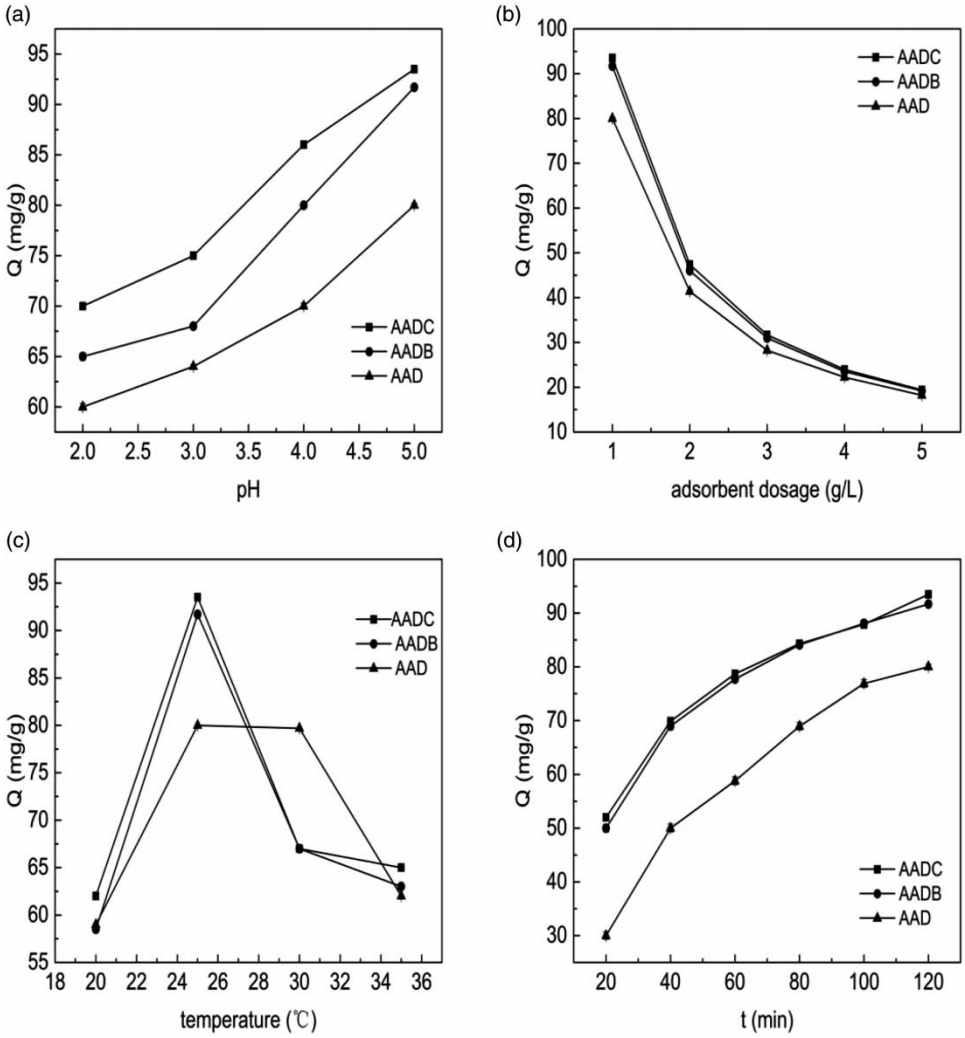

Figure 1 | (a) Effect of solution pH on Cd(II) biosorption (25 °C, 150 r/min, adsorbent dosage of 1 g/L, biosorption time of 120 min, Cd(II) initial concentration of 100 mg/L); (b) Effect of adsorbent dosage on Cd(II) biosorption (25 °C, 150 r/min, biosorptiontime of 120 min, pH 5, Cd(II) initial concentration of 100 mg/L); (c) Effect of temperature on Cd(II) biosorption (adsorbent dosage of 1 g/L, 150 r/min, pH 5, biosorption time of 120 min, Cd(II) initial concentration of 100 mg/L); and (d) Effect of biosorption time on Cd(II) biosorption (25 °C, adsorbent dosage of 1 g/L, 150 r/min, pH 5, Cd(II) initial concentration of 100 mg/L).

of AAD by 14.4% and 12.7%, respectively. The effect of solution pH on biosorption efficiency was correlated with the participation of functional groups in the adsorption (Nomanbhay & Palanisamy 2004). From the FTIR analyses, it could be seen that AADC and AADB had more functional groups than AAD. In the same time, from the later results analysis of biosorption mechanism, it also could be concluded that composting and pyrolysis had a great influence on AAD, which could make more active sites exposed to adsorb Cd(II). At low pH, more H^+ occupied biosorption sites on the adsorbent surface rather than Cd(II); when pH rose, more negatively charged groups appeared on the adsorbent surface and more Cd(II) ions were adsorbed.

Effect of adsorbent dosage

The adsorbent dosage determines the amount of active sites for Cd biosorption and directly affects the biosorption quantity. From Figure 1(b), when the adsorbent dosage ascended from 1 g/L to 5 g/L, the biosorption quantity of AADC decreased from 93.5 mg/g to 19.4 mg/g, and that of AADB from 91.7 mg/g to 19.2 mg/g, but both were higher than that of AAD at corresponding dosage (from 80.0 mg/g to 18.2 mg/g). No matter what the dosage was, the adsorption quantity of AADC and AADB was higher than that of AAD. When the adsorbent dosage increased, overlap and polymerization occurred between the adsorbents. When the adsorbent overlapped or polymerized, the effective sites

Downloaded from http://iwa.silverchair.com/wst/article-pdf/79/8/1511/617908/wst079081511.pdf
by guest

with ion exchange activity were also reduced, resulting in a decreased biosorption (Huang *et al.* 2008; Hu *et al.* 2014). For AADB and AADC, pyrolysis and composting could provide more hydrogen and ammonia than AAD, more adsorbent dosage meant more hydroxide and ammonia which was helpful to adsorb Cd(II). Considering the effect of adsorbent dosage on the biosorption quantity, this experiment selected the adsorbent dosage of 1 g/L for subsequent experiments.

Effect of temperature

Since biosorption process might involve both endothermic and exothermic process, the temperature must be an important factor in Cd(II) biosorption. In this study, the biosorption quantities of three adsorbents were all increased rapidly (62.0 mg/g to 93.5 mg/g, 58.5 mg/g to 91.7 mg/g and 59.0 mg/g to 80.0 mg/g for AADC, AADB and AAD, respectively) as temperature elevated from 20 °C to 25 °C. This might be due to the presence of chemisorption during the biosorption process. Chemisorption is an endothermic process in which the system absorbs heat from surroundings, therefore higher temperature favors the occurrence of this process. When the temperature rose, the ion velocity of the solution increased, accelerating the diffusion of the adsorbent, and promoting the effective collision between the metal ions and the adsorbent surface (Kumar & Chakraborty 2009; Kumar *et al.* 2011). When the temperature rose from 25 °C to 35 °C, the biosorption quantity of the three adsorbents were all decreased from 93.5 mg/g to 65.0 mg/g, 91.7 mg/g to 63.0 mg/g and 80.0 mg/g to 62.0 mg/g for AADC, AADB and AAD, respectively. This might be due to the presence of physical process during the biosorption. The physical biosorption mainly carried out at a low temperature, and the desorption might occur with the increase of temperature (Lodeiro *et al.* 2006; Luo *et al.* 2011). Obviously, the maximum biosorption quantity for each biosorbent was obtained at 25 °C in the order of AADC > AADB > AAD. However, there was one point to note that when temperature ascended to 30 °C, the biosorption quantity of AAD only changed slightly.

Effect of biosorption time

The effect of biosorption time is shown in Figure 1(d). From 20 min to 120 min, the biosorption quantities of AADC, AADB and AAD were increased from 52.0 mg/g to 93.5 mg/g, 50.0 mg/g to 91.7 mg/g, and 30.0 mg/g to 80.0 mg/g, respectively. It could be seen clearly that the variation tendency of biosorption quantities of AADC and AADB were more alike. And the maximum biosorption quantities of AADC and AABD were 14.4% and 12.7% higher than that of AAD, respectively. The adsorption efficiency of AADB and AADC was better than that of AAD; the reason might be that many basic properties such as specific surface area, porosity, element content and functional groups were changed during pyrolysis and composting. These were mentioned in the analyses of the following mechanisms. From the figure, it can be deduced that the sorption speed in the early stage was fast, and it gradually slowed down in the later stage. This was mainly due to the mass transfer impetus that resulted from the difference in Cd(II) concentration on the adsorbent surface and in the solution, which facilitated the ion exchange. With the progress of biosorption, the differential between the concentration of Cd(II) gradually narrowed and the biosorption sites for Cd(II) to occupy also reduced, resulting in a slower biosorption rate and a final biosorption equilibrium.

Biosorption isotherms

The isothermal model can be used to estimate the affinity between the adsorbate and the adsorbent and describe the surface characteristics of the adsorbent (Tan & Xiao 2009). The Langmuir isotherm model is derived from the assumption of monolayer biosorption between gas and solid phases, which is commonly used to determine the adsorption properties of metal ions at the interface of solid materials (Vimala & Das 2009). The Freundlich isotherm biosorption model is commonly used in the biosorption process of inorganic or organic matter to simulate the biosorption under irrational conditions and the multilayer biosorption mechanism (Torab-Mostaedi *et al.* 2013). As seen from Figure 2 and Table 1, the experimental data of the three adsorbents conformed to both Langmuir and Freundlich models, indicating that monolayer biosorption and multilayer biosorption coexisted in these biosorption processes. And the higher R^2 value of the Langmuir model indicated that the Langmuir model was better to describe the biosorption and monolayer biosorption might dominate the process. According to the average biosorption energy (E) given in Table 1, it was inferred that the biosorption process was mainly chemibiosorption (Oguz 2005). Meanwhile, based on Langmuir model, the theoretical maximum biosorption quantity for Cd(II) of the three biosorbents was AADC > AADB > AAD. A comparison of biosorption quantity between other adsorbents and the three adsorbents is shown in Table 2, apparently, though the biosorption

Downloaded from http://iwa.silverchair.com/wst/article-pdf/79/8/1511/617908/wst079081511.pdf
by guest

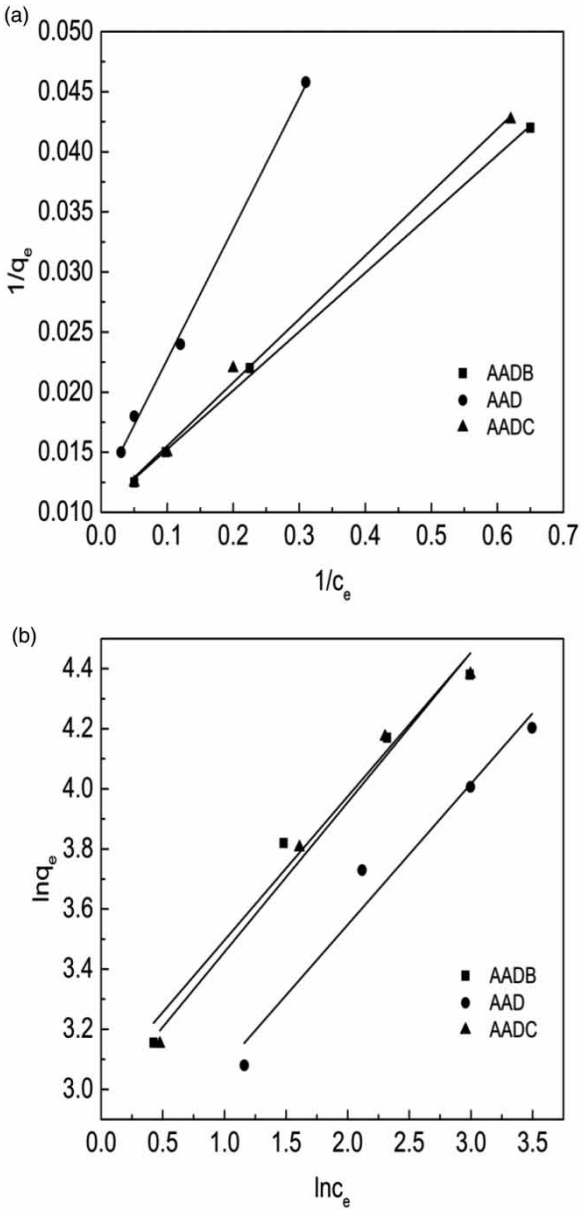

Figure 2 | Langmuir (a), Freundlich (b) and isotherm models for Cd(II) biosorption.

quantity of AAD was 14.0% and 15.2% lower than that of AADB and AADC, respectively, they were all higher than that of other adsorbents, indicating the *Auricularia auricula* dreg derived adsorbents performed better in the biosorption of Cd(II).

Table 1 | Parameters of Langmuir and Freundlich isotherm models

Models		AAD	AADB	AADC
Langmuir	q_{max} (mg/g)	84.6	96.5	97.5
	K_L (L/mg)	0.109	0.212	0.194
	R^2	0.9964	0.9985	0.9949
Freundlich	n	2.17	2.13	2.04
	K_F (mg/g)/(mg/L)$^{1/n}$	13.589	20.436	19.265
	R^2	0.9503	0.9659	0.9770

Table 2 | Q_{max} of various adsorbents for Cd(II) biosorption

Adsorbent	Q_{max}(mg/g)	Reference
S. platensis	73.6	Çelekli & Bozkurt (2011)
Pomelo peel	21.8	Njoku *et al.* (2012)
Ceramium virgatum	39.7	Sari & Tuzen (2008)
Waste tea leaves	31.5	Tee & Khan (1988)
Chlorella vulgaris	85.3	Aksu (2001)
Chlamydomonas reinhardtii	42.6	Tuzun *et al.* (2005)
Olive cake	65.4	Panda *et al.* (2007)
Nile water algae	29.6	Wang *et al.* (2007)
AAD	84.6	This study
AADB	96.5	This study
AADC	97.5	This study

Biosorption kinetics

The pseudo-first-order kinetic and pseudo-second-order kinetic models were used to illustrate the kinetic characteristics of Cd(II) biosorption by the three biosorbents. As shown in Figure 3 and Table 3, the R^2 values of pseudo-second-order kinetics were greater than the those of pseudo-first-order kinetics, indicating that the biosorption process of the three adsorbents was more suitable for the pseudo-second-order kinetic model. Compared with the R^2 values of pseudo-first-order kinetics of AAD(0.9344), that of AADB(0.8494) and AADC(0.8024) were lower clearly. This might be due to composting and pyrolysis causing changes in the surface functional groups of the adsorbent, resulting in changes in functional groups involved in biosorption.

The biosorption quantity of AAD, AADB and AADC obtained by pseudo-first-order kinetics was about 147.6 mg/g, 149.1 mg/g, 126.4 mg/g, respectively, while that obtained by pseudo-second-order kinetics was about 121.9 mg/g, 109.0 mg/g and 106.6 mg/g, which closer to that obtained from this experiment. Considering the results from isotherm and kinetic models, it could be deduced that the biosorption process was mainly dominated by a chemical process (Harja *et al.* 2012).

Thermodynamic modeling

As the result shows in Table 4, ΔG^0 values of the three adsorbents were all less than 0 which indicated that

Downloaded from http://iwa.silverchair.com/wst/article-pdf/79/8/1511/617908/wst079081511.pdf
by guest

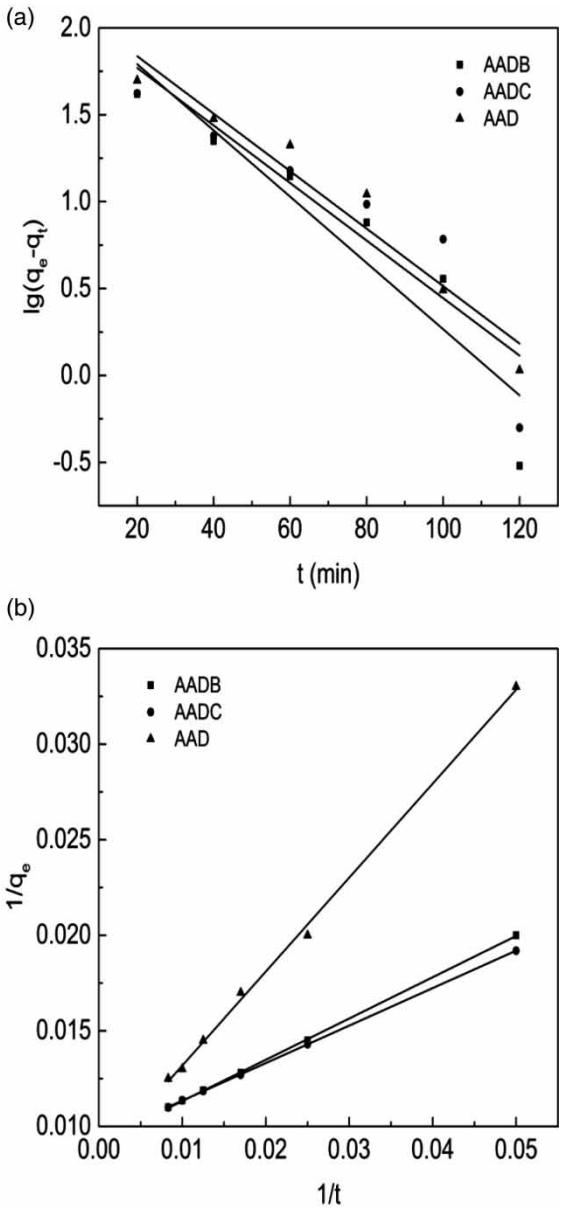

Figure 3 | Pseudo-first-order (a) and pseudo-second-order (b) kinetic model plot for Cd(II) biosorption.

the biosorption reaction was spontaneous. The smaller the Gibbs free energy, the greater the spontaneity of the reaction. From Table 4, it can be seen that the spontaneity of the three adsorbents was in the order of AADC > AADB > AAD.

Biosorption mechanism

SEM-EDX analyses

The surface morphology of different adsorbents was observed under a scanning electron microscope at a magnification of 500 times. As seen in Figure 4, the surface of AAD had an irregularly lamellar and porous structure. These special structures would provide AAD the ability to adsorb heavy metals. Both AADC and AADB exhibited a relatively regular porous structure, and AADB had some tubular structures around the pores on its surface, which might be caused by the collapse of structures such as lignocellulose during carbonization (Park *et al.* 2015). It is these structures that give them good adsorption efficiency.

The elemental composition of three adsorbents are shown in Table 5. The relative weight (in percent) of C of AADB was obviously higher than that of AADC and AAD, but that of N and O were obviously less than that of AADC and AAD, which might be due to the dehydration of hemicellulose, cellulose, lignin and other substances, the polycondensation of aromatic ring into carbon, and the release of volatile organic compounds. It could also be seen from the XRD analysis that a large amount of nitrate-containing substances existed on AADC after composting, which was also the reason for the increase in the content

Table 4 | ΔG^0 for Cd(II) biosorption onto three adsorbents

Thermodynamic parameter	AAD	AADB	AADC
ΔG^0 (kJ/mol)	−3.435	−5.952	−6.606

Table 3 | Parameters of two kinetic models

Adsorbents	Experimental q_e (mg/g)	Pseudo-first-order kinetics			Pseudo-second-order kinetics		
		k_1 (1/min)	q_e (mg/g)	R^2	k_2 (g/mg min)	q_e (mg/g)	R^2
AAD	80.0	0.038	147.6	0.9344	0.141×10^{-3}	121.9	0.9977
AADB	91.7	0.044	149.1	0.8494	0.389×10^{-3}	109.0	0.9998
AADC	93.5	0.0381	126.4	0.8024	0.454×10^{-3}	106.6	0.9997

Downloaded from http://iwa.silverchair.com/wst/article-pdf/79/8/1511/617908/wst079081511.pdf
by guest

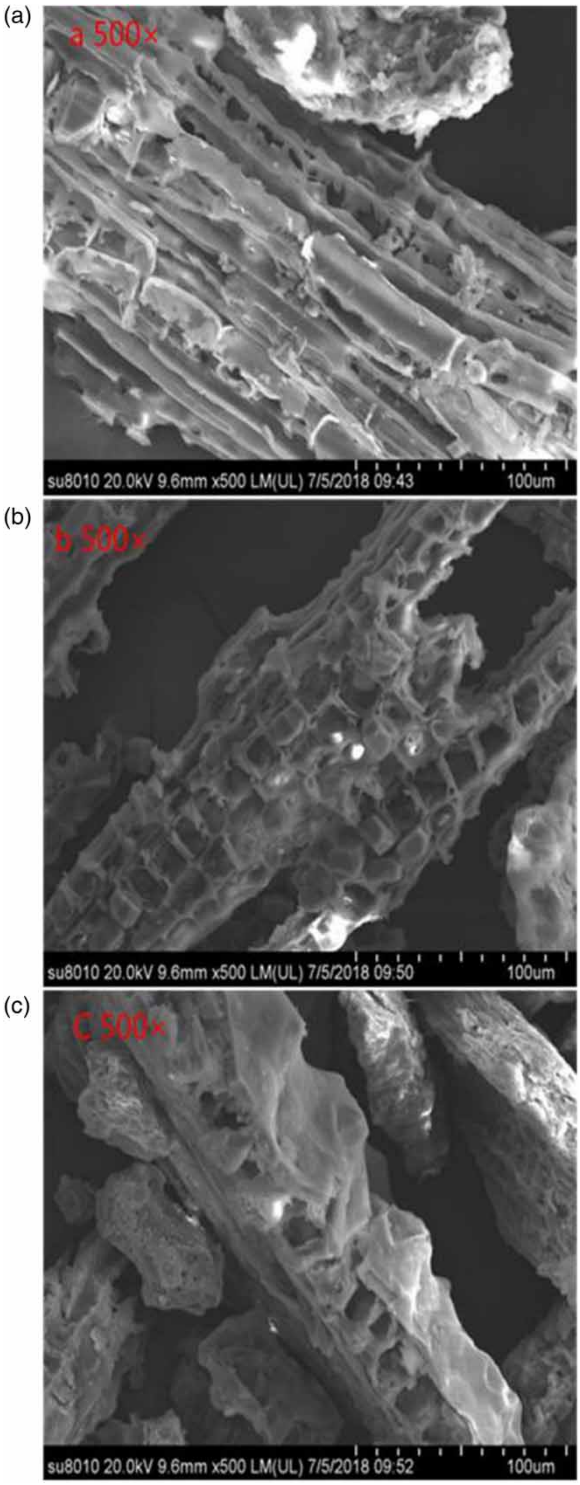

Figure 4 | SEM images of the three adsorbents: (a) AAD, (b) AADB, and (c) AADC.

of N. After biosorption, the content of Na, Mg, Al and Si for the three adsorbents were all increased, and Cd(II) appeared on the biosorbents after biosorption. The relative weight (in percent) of Cd on AADC was obviously higher than that on AADB and AAD. This was in line with the results of the batch biosorption experiments that the biosorption efficiency of AADC was higher than that of AADB and AAD.

Table 5 | Elemental composition of three adsorbents

	AAD (Wt%)		AADB (Wt%)		AADC (Wt%)	
Element	Native AAD	AAD-Cd	Native AADB	AADB-Cd	Native AADC	AADC-Cd
C	41.94	47.69	49.13	52.34	26.54	32.07
N	11.55	9.73	14.03	9.57	18.98	19.34
O	37.48	35.89	30.04	25.88	42.68	26.24
Na	0.87	1.45	0.92	1.20	1.70	1.87
Mg	0.48	0.54	0.74	1.03	1.00	1.15
Al	0.45	0.37	0.06	0.24	0.27	1.90
Si	0.61	0.83	0.34	1.92	1.60	2.28
P	0.07	0.00	1.71	1.13	0.43	2.51
Cl	0.06	0.04	0.17	0.05	0.57	0.09
K	0.12	0.00	2.04	0.54	1.11	1.26
Ca	1.03	0.57	0.09	3.72	1.11	3.94
Pt	5.34	2.09	0.73	1.49	4.01	4.15
Cd	0.00	0.80	0.00	0.89	0.00	3.20

FTIR analyses

The FTIR profiles and functional groups of three biosorbents before and after biosorption are given in Figure 5 and Table 6. It could be seen clearly that all three adsorbents contained -OH, CO_3^{2-} and PO_4^{3-}. For AAD, there were C = O and -NH presented at the peak of 1,620 cm^{-1} and 1,480 cm^{-1}, but the peak intensity was not strong, indicating that the number of functional groups involved in biosorption was not as great as that in AADC. For AADB, the intensity of the peaks in the range of 800–1,500 cm^{-1} was obviously stronger than those of other two adsorbents which indicated this region contained relatively abundant functional groups and might play a major role in the biosorption process. The functional groups involved in biosorption were mainly CO_3^{2-}, -C-O-C- and PO_4^{3-}. It also could be seen clearly from Table 6 that compared with the other two adsorbents, AADB lacked many functional groups, such as -CH and -NH which might be caused by pyrolysis (Baldock & Smernik 2002) which was one of the reasons why its adsorption efficiency was not as good as AADC. For AADC, the peaks near 2,900–3,000 cm^{-1} were symmetric or asymmetric C-H and $-CH_2$ stretching vibration of aliphatic

Downloaded from http://iwa.silverchair.com/wst/article-pdf/79/8/1511/617908/wst079081511.pdf
by guest

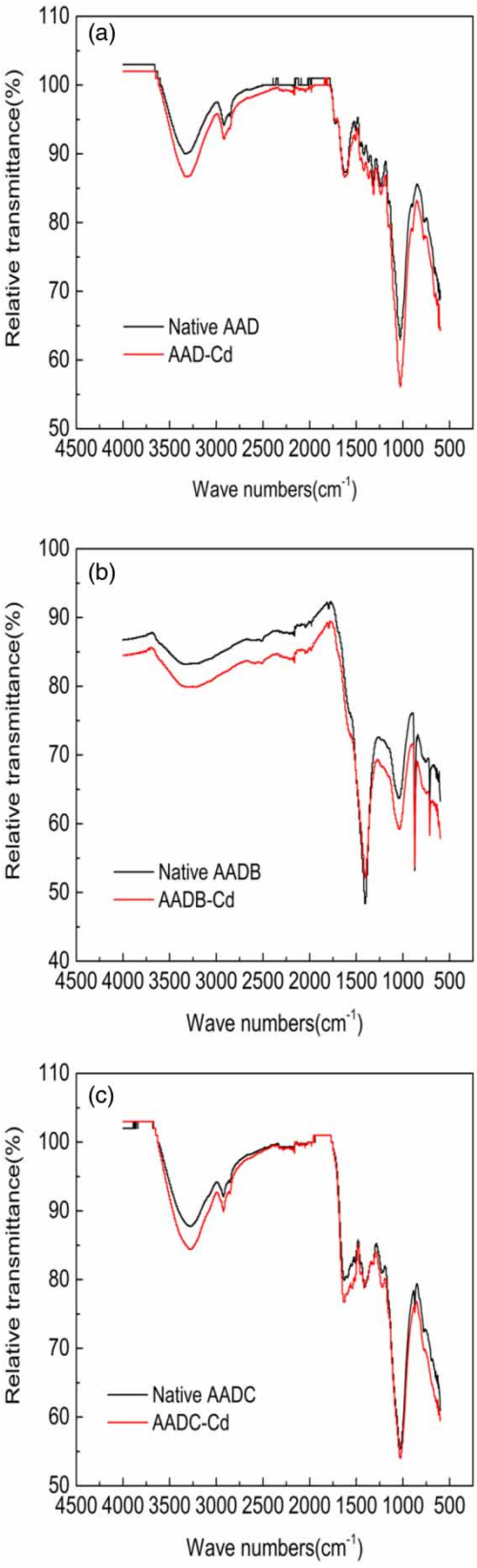

Figure 5 | FTIR images of three adsorbents: (a) AAD, (b) AADB, and (c) AADC.

acids. The diffuse peak near 3,280 cm^{-1} was derived from the broad peak of stretching vibration of -OH. The absorption peak shifted after biosorption indicated its involvement in the biosorption reaction. The diffuse peak near 1,480 cm^{-1} and 1,620 cm^{-1} were the stretching vibration of -NH and the peak near 1,620 cm^{-1} was C = O absorption peak in carboxyl group and ketone. After biosorption, they all had a significant changes in vibration frequency which might be due to surface biosorption and complexation (Tan & Xiao 2009). Compared with AAD, the increased intensity of -NH in AADC might be the conversion of inorganic ammonia to organic ammonia during composting (Rumapar *et al.* 2013). As described above, the difference in functional groups contained in the three adsorbents has a great influence on the adsorption of cadmium, which could explain the results of the batch biosorption experiments. As shown in Figure 5, with the peaks before and after the adsorption were compared, it could be seen from FTIR image that the intensity of the characteristic peaks of the three adsorbents changed greatly before and after biosorption, indicating that chemical changes including redox, ion exchange, and coordination might occur during the whole process. And the positional shifts and the generation of new peaks indicated that these biosorptions were all a combination of physical and chemical processes.

XRD analyses

A difference of the XRD profile of AADC, AADB and AAD before and after biosorption is shown in Figure 6 and the details of crystalline species are given in Table 7. All three adsorbents had a broad peak at the 2θ of 20–30°, which represented that these materials contained a high content of cellulose. As for AAD, the sharp peak at the 2θ about 14.437° was the crystal of CH_4N_2O!$C2H_2O$. At the peaks around 21–23°, there was a broad peak which represented $Na_2Mg(PO_3)_4$, $Ca_2Fe(CN)_6$ and $Ca(NO_2)_2$ and so on. As for AADB, the peaks at the 2θ about 29.062° and 26.212° represented $FeSi_2$ and $CaCO_3$, respectively, which were not available in AAD. As for AADC, there was a sharp peak at the 2θ about 26° and the major crystalline species was SiO_2 which played an important role in the complexation and coordination of metal ions. Compared with AAD, there were many new peaks appeared, the elements contained in the substances represented by these peaks could also be seen in the elemental analysis. After the biosorption, the new peak at 2θ about 30.063° representing $Cd_4P_2O_9$ appeared on AAD, indicating that Cd was well adsorbed. Compared with two other adsorbent materials,

Downloaded from http://iwa.silverchair.com/wst/article-pdf/79/8/1511/617908/wst079081511.pdf
by guest

Table 6 | The wavenumbers and functional groups of three adsorbents

AAD wavenumber (cm^{-1})		AADB wavenumber (cm^{-1})		AADC wavenumber (cm^{-1})		
Native AAD	**AAD-Cd**	**Native AADB**	**AADB-Cd**	**Native AADC**	**AADC-Cd**	**Functional groups**
3,315	3,310	3,323	3,324	3,280	3,290	-OH (Lin *et al.* 2012)
2,990	2,984	absent	absent	3,000	2,990	-CH (Safari *et al.* 2013)
1,490	1,490	absent	absent	1,480	1,490	-NH (Wahab *et al.* 2010)
852	852	867	875	871	873	CO_3^{2-} (Kalinke *et al.* 2016)
1,406	1,408	1,398	1,399	1,410	1,413	
1,620	1,621	absent	absent	1,620	1,625	C = O of COOH and -NH (Wahab *et al.* 2010)
absent	1,820	1,805	1,804	absent	absent	C = O (Li *et al.* 2007)
1,030	1,030	1,032	1,032	1,030	1,028	PO_4^{3-} and Si-O-Si (Kalinke *et al.* 2016)
absent	absent	1,256	1,260	absent	absent	-C-O-C-
2,920	2,920	absent	absent	2,920	2,920	-CH (Safari *et al.* 2013)

AAD was obviously missing some sharp peaks which can be seen in Figure 6. The absence of these sharp peaks might indicate that AAD lacked some functional groups than the other two adsorbents. This also explained why the biosorption efficiency of AAD was not as good as that of the other two adsorbents. After biosorption of AADB, the XRD diffraction peak did not change much, which can be clearly seen from Figure 6. From Table 7, it can be seen that after biosorption, the major crystalline species also lacked hydroxyl groups compared with AADC. After the biosorption of Cd(II) for AADC, various compounds containing Cd were present. These compounds had various groups such as hydroxyl, nitro, amino and phosphate groups. As above, it explained why the biosorption performance of AADC was better than that of AADB and AAD.

XPS analyses

The XPS scanning spectra of the three adsorbents after Cd^{2+} biosorption are shown in Figure 7. C 1s, N 1s and O 1s were the main peaks detected in the biomass spectrum. As shown in Figure 7, for the three adsorbents, the deconvolution of the C 1s spectra yielded peaks with corresponding binding energies of 284.8 eV for C-C and C-H species, 285.6 eV for C-N species, 286.3 eV for -C = N or C-OH species (Zhou *et al.* 2007). While for AADC, a peak at 287.3 eV which represented -C = O appeared. The deconvolution of the N 1s spectra yielded peaks with corresponding binding energies of 401.58 eV for NH_4^+ species, and new decomposed peaks with binding energy of 399.1 eV for -CN species and 399.73 eV for -NH species appeared in AAD and AADC (Pels *et al.* 1995). The increased intensity of -NH in AADC might be the conversion of inorganic ammonia to organic ammonia during composting which was consistent with the results of FTIR. The deconvolution of the O 1s spectra yielded peaks with corresponding binding energies of 531.0 eV for carbonyl oxygen of quinines, 532.6 eV for carbonyl oxygen atoms in esters, anhydrides and oxygen atoms in hydroxyl groups (Lakshminarayanan *et al.* 2004). Some new decomposed peaks (533.1 eV for -COO- and 534.3ev for -COOH) appeared in AAD and AADC. It could be seen clearly from the picture that the deconvolution spectra of each adsorbent was different in the peak of Cd 3d after Cd(II) adsorption, two peaks were observed on AADC, indicating the existence of two Cd chemical states with different binding energies. The Cd 3d peak of binding energy 405.99 eV could be attributed to the formation of an ester–cadmium complex (Sheng *et al.* 2004).

BET surface area, particle size, pH, Zeta potential, CEC and oxygen-containing functional groups

The BET surface area and the particle size are of great importance to the performance of adsorbents, because they determine the physical biosorption capacity of the biosorbents. As shown in Table 8, the surface area of AAD, AADB, AADC was 50.32 m^2/g, 58.64 m^2/g and 40.32 m^2/g, respectively. The increased surface area of AADB might be due to the vanishing of a large amount of volatile components in the dreg and the formation of more pore structure during the pyrolysis process, while the decreased surface area of AADC might be ascribed to the substances produced during composting blocked relatively small pores. As shown in Table 8, the total pore volume of

Downloaded from http://iwa.silverchair.com/wst/article-pdf/79/8/1511/617908/wst079081511.pdf
by guest

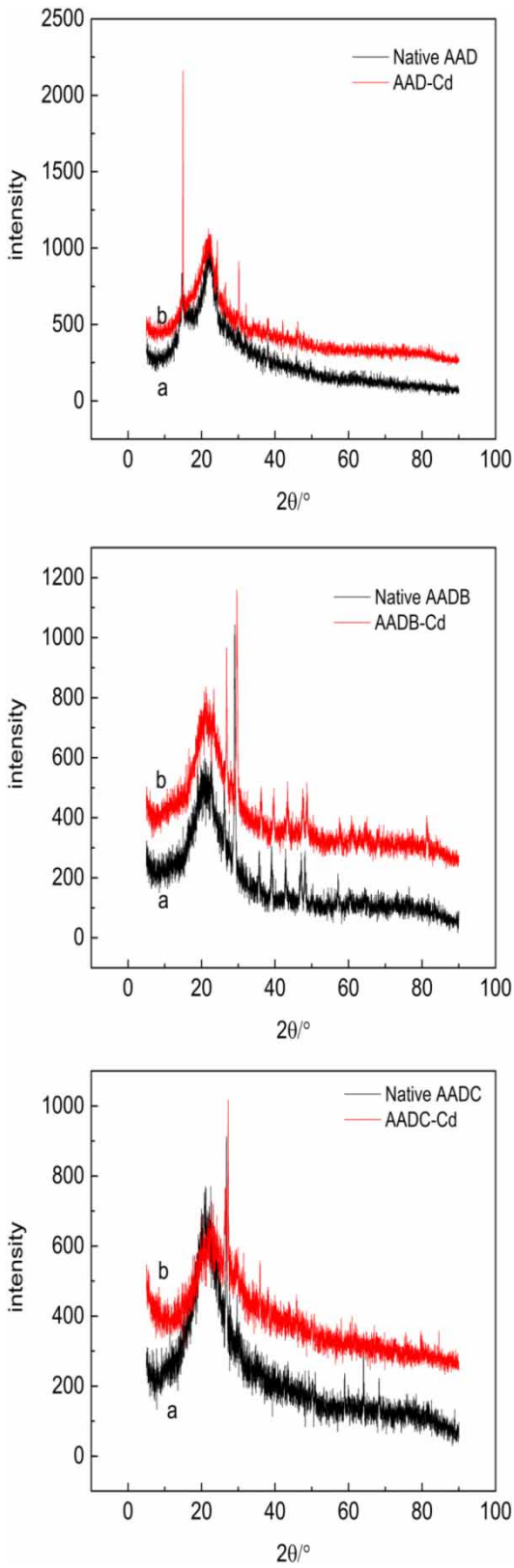

Figure 6 | XRD diffraction peaks of three adsorbents (a were the native adsorbents; b were the adsorbents-Cd).

the three adsorbents was in the following order: AADC > AADB > AAD, which illustrated that AADC and AADB had better porosity than AAD, this result was consistent with that observed by electron microscopy.

The pH value of the adsorbents was determined by the national standard method. 2.50 g of biochar sample was weighed and placed in a 100 mL conical flask. Deionized water without CO_2 was added (boiled by boiling method, that is, the deionized boil to volume reduction), 10% or more, capped with cold water is 50 mL without CO_2 pure water, heated, gently boiled for 5 min, filtered, the primary filtrate was discarded, and the remaining liquid was cooled to room temperature, and the pH value was measured by pH meter. As shown in Figure 8, there are a lot of negative charges on the surface of AADC and AADB and the pHPZC of AAD, AADB and AADC were 3.10 mV, 2.19 mV and 2.02 mV, respectively. When the pH was 5, AADC had more negative charges which was beneficial to adsorb mental cations. The low isoelectric point of compost might be due to the existence of a large number of negative charges and quaternary amine functional groups on the surface of the compost. Because Cd(II) is cationic, a negatively charged adsorbent may be more effective in adsorbing it, which also explains that the AADC described above had the best adsorbing effect. The CEC and pH value of three adsorbents are shown in Table 9. It can be seen from Table 9 that the pH values of all three adsorbents were weakly alkaline and in the order of AADC > AADB > AAD. The higher the pH, the more negative the charge on the adsorbents and the higher the biosorption efficiency for cations (Gómez-Brandón *et al.* 2008). Based on the above experimental results, it could also be deduced that the AADC might have the best biosorption for Cd(II), which had been corroborated by the batch experiments.

The adsorbent with more oxygen-containing functional groups on its surface generally has a higher CEC (Liang *et al.* 2006). Besides the properties of adsorbent itself, the pH value of adsorbent also affects its CEC (Cheng *et al.* 2014). From Table 9, it can be seen clearly that all three adsorbents showed higher CEC. The CEC of AADB (62 cmol kg^{-1}) and AADC (73 cmol kg^{-1}) were obviously higher than that of AAD (43 cmol kg^{-1}) by 30.6% and 41.1%. High cation exchange capacity leads to good adsorption efficiency of the adsorbent. The CEC of AAD, AADB and AADC in Table 9 could explain that AADB and AADC have better adsorption efficiency than AAD in the previous batch biosorption experiments.

Mix 0.1 g of adsorbent sample 20 mL of solution containing 0.1 mol·L^{-1} of NaOH, 0.05 mol·L^{-1} of Na_2CO_3

Downloaded from http://iwa.silverchair.com/wst/article-pdf/79/8/1511/617908/wst079081511.pdf
by guest

Table 7 | The crystalline species of the three adsorbents before and after biosorption

AAD				AADB				AADC			
Native AAD		AAD-cd		Native AADB		AADB-Cd		Native AADC		AADC-Cd	
2θ	Crystalline species	2θ	Crystalline species	2θ	Crystalline species	2θ	Crystalline species	2θ	Crystalline species	2θ	Crystalline species
23.266	$Na_2Mg(PO_3)_4$	15.060	$(NH_4)_8P_6O_{19}!2H_2O$	15.003	$C_4H_4CuO_6!3H_2O$	26.831	$C_2H_2CaO_4$	21.238	$MgAl_2O_4!7.9H_2O$	27.165	$CH_6N_2O_2!0.5H_2O$
14.437	$CH_4N_2O!C2H_2O_4$	15.029	$Mg_5(CO_3)_4(OH)_2!8H_2O$	17.796	$CH_6N_2O_2!0.5H_2O$	29.756	$(NH_4)2CO_3!H_2O$	29.395	$Na_2CO_3!10H_2O$	17.894	$Cd(OH)_2$
26.243	SiO_2	15.588	$C_4H_{10}CdN_4O_6$	17.408	$Fe_2O_2CO_3$	29.198	$2NH_3!H_2O$	29.454	$FeSiO_3$	17.724	$Cd(NO_3)_2!4H_2O$
25.651	$Ca_5(SiO_4)2CO_3$	30.063	$Cd_4P_2O_9$	35.597	CaO_2	29.766	$(NH_4)HCO_3$	26.708	SiO_2	29.062	$C_2H_2O_4!2H_2O$
24.231	C_2CaO_4	24.366	$Al_{1.4}Si_{0.3}O_{2.7}$	35.743	MgC_2	19.823	$C_2H_2CdO_4!2H_2O$	19.364	$CH_4N_2O!C_2H_2O_4$	29.756	$(NH_4)_2CO_3!H_2O$
19.936	$Si_{1.8}Al_{0.2}O_{1.2}N_{1.8}$	22.032	SiO_2	35.743	$Fe_{2.35}Si_{0.65}O_4$	24.195	$C_4H_{16}N_8O_4!Ca(NO_3)_2$	24.366	$C_6H_9AlO_6$	29.655	$C_2H_8N_2O_4$
22.980	$C_{11}PF_6$	30.420	$MgCO_3!2H_2O$	28.755	$CH_4N_2O!HNO_3$	19.900	$Cd(CN)_2$	29.756	$(NH_4)2CO_3!H_2O$	19.924	SiO_2
24.032	$H_4P_2O_6!2H_2O$	14.970	$NH_4N(NO_2)_2$	29.159	$Ca(N_3)_2$	20.305	$Cd(NO_3)_2$	26.667	$C_2H_2MgO_4!2H_2O$	21.830	$C_3H_3AlO_6!CH_2O_2$
26.667	$NH_2NH_2!HNO_3$	27.681	$Na_7[Al_5Si_7O_{24}]CO3!3H_2O$	20.465	Na_6C_{60}	23.707	$C_2CdO_4!3H_2O$	23.334	$C_{12}PF_{5.5}$	26.997	NH_4Cl
22.319	CH_4N_2O	22.606	$Cd(PO_3)_2$	21.604	SiO_2	15.290	$Mg_5(CO_3)4(OH)_2!4H_2O$	22.237	CH_4N_2O	15.290	$(NH_4)2Fe_2(OH)_4(CO_3)_2!H_2O$
21.341	$Ca_2Fe(CN)_6$	26.466	$Cd(OH)NO_3!H_2O$	25.502	CaN_2O_3	29.454	$FeSiO_3$	18.126	$C_2MgO_4!2H_2O$	23.266	$Mg(NH_2)_2$
21.604	$Ca(NO_2)_2$	30.484	$CH_6N_2O_2!0.5H_2O$	29.062	$FeSi_2$	19.364	$CH_4N_2O!C2H_2O_4$	19.999	$Mg(NO_3)_2!6H_2O$	19.823	$C_2H_2CdO_4!2H_2O$
				26.212	$CaCO_3$	27.039	$Mg(NO_3)_2!6H_2O$	29.454	$Al(NO_3)_3!9H_2O$	20.639	$C_20H_{52}N_4!88SiO_2$
				35.597	$Fe_{1.6}SiO_4$	26.955	$Cd_3(PO_4)_2$	27.857	$Ca(N_3)_2!0.5H_2O$	24.098	$C_4H_7AlO_5!2.5H_2O$
				26.667	$NH_2NH_2!HNO_3$	21.604	SiO_2	26.831	$NH_3!H_2O$	21.841	$C_2H_7NO_2$

Downloaded from http://iwa.silverchair.com/wst/article-pdf/79/8/1511/617908/wst079081511.pdf
by guest

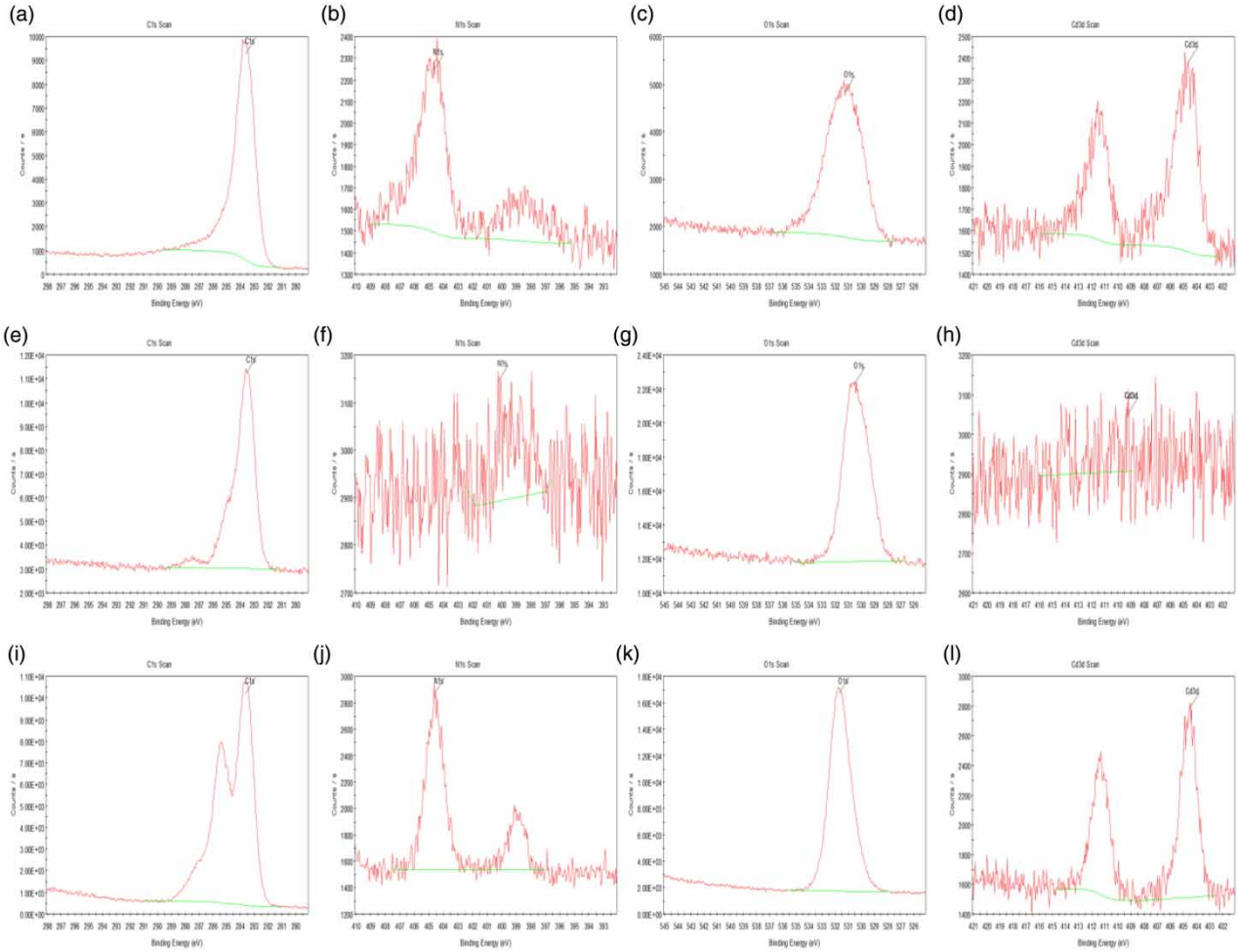

Figure 7 | XPS spectra of AAD ((a) C 1s (b) N 1s (c) O 1s (d) N 1s), AADB ((e) C 1s (f) N 1s (g) O 1s (h) N 1s), AADC ((i) C 1s (j) N 1s (k) O 1s (l) N 1s).

Table 8 | BET characteristics of AADC, AADB and AAD

Adsorbent	BET surface area (m^2/g)	Total pore volume (cm^3/g)	Average pore diameter (Å)	Micropore volume (cm^3/g)	Middle pore volume (cm^3/g)
AAD	50.32	0.0534	46.98	0.0255	0.0154
AADB	58.64	0.0612	48.37	0.0392	0.0235
AADC	40.32	0.0832	50.21	0.0551	0.0286

and 0.1 mol·L^{-1} of $NaHCO_3$), after shaking at 25 °C and 160 r/min for 24 h. The mixture was filtered, and supernatant was reacted with 0.1 mol·L^{-1} HCl solution with bromocresol green-methyl red as indicator. Table 10 lists the amounts of functional groups in three adsorbents determined by Boehm titration method. The content of acidic functional groups in AADC was 2.02 mmol/g, which was 9.41% and 22.77% higher than that of AADB and AAD,

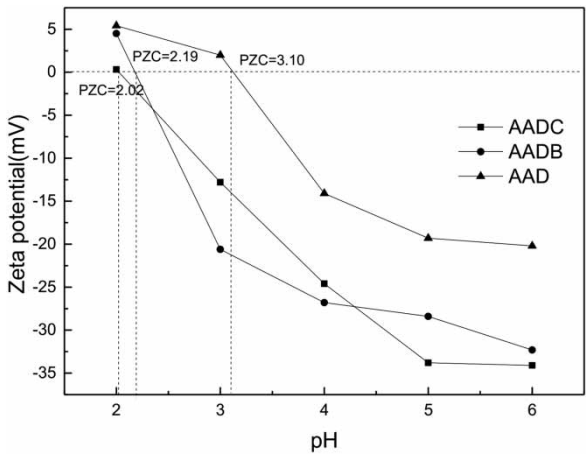

Figure 8 | Zeta potential.

respectively, indicating that AADC probably had the largest cation exchange capacity and the strongest hydrophilicity

Downloaded from http://iwa.silverchair.com/wst/article-pdf/79/8/1511/617908/wst079081511.pdf
by guest

Table 9 | CEC and pH of three adsorbents

	AAD	AADB	AADC
CEC (cmol kg^{-1})	43	62	73
pH	7.37	7.83	8.64

Table 10 | Oxygen-containing functional groups of three adsorbents

Adsorbent	Acidic functional group (mmol/g)	Carboxyl (mmol/g)	Phenolic hydroxyl (mmol/g)	Lactone group (mmol/g)
AAD	1.56	0.71	0.32	0.53
AADB	1.83	0.82	0.37	0.64
AADC	2.02	0.68	0.55	0.79

among the three adsorbents. This was also in line with the previous description. It can also be seen from Table 10 that these acidic functional groups were mainly composed of carboxyl groups, phenolic hydroxyl groups and lactone groups. And the number of carboxyl groups and lactone groups were substantially more than that of phenolic hydroxyl groups.

CONCLUSIONS

Batch biosorption experiments screened the best biosorption conditions which were adsorbent dosage of 1 g/L, pH at 5.0, biosorption temperature of 25 °C, and biosorption time of 120 min, respectively. The maximum biosorption quantity of the three adsorbents was in the following order: AADC > AADB > AAD. From the previous results, it could be seen that composting and pyrolysis did not affect the isotherm and kinetic experiments. According to the Langmuir model and pseudo-second-order model, the biosorption of Cd(II) onto three adsorbents was mainly a chemical process and occurred on a homogeneous and monolayer surface, and also spontaneously by analyses of thermodynamic. Through the analysis of the biosorption mechanism, it could be concluded that composting and pyrolysis had a huge impact on the structure and composition of the AAD, which had an impact on the biosorption process.

ACKNOWLEDGEMENTS

This work was financially supported by the National Key Research Project of China (Grant number: 2017YFD0801104).

REFERENCES

Aksu, Z. 2001 Equilibrium and kinetic modelling of cadmium (II) biosorption by *C. vulgaris* in a batch system: effect of temperature. *Separation and Purification Technology* **21**, 285–294.

Baldock, J. A. & Smernik, R. J. 2002 Chemical composition and bioavailability of thermally altered *Pinus resinosa* (red pine) wood. *Organic, Geochemistry* **33**, 1093–1109.

Bayo, J. 2012 Kinetic studies for Cd(II) biosorption from treated urban effluents by native grapefruit biomass (*Citrus paradisi* L.): the competitive effect of Pb(II), Cu(II) and Ni(II). *Chemical Engineering Journal* **191**, 278–287.

Çelekli, A. & Bozkurt, H. 2011 Bio-sorption of cadmium and nickel ions using *Spirulina platensis*: kinetic and equilibrium studies. *Desalination* **275**, 141–147.

Chen, A. H. & Chen, S. M. 2009 Biosorption of azo dyes from aqueous solution by glutaraldehyde-crosslinked chitosans. *Journal of Hazardous Materials* **172** (2–3), 1111–1121.

Cheng, S., Yang, Z., Wang, M. J., Song, J., Sui, N. & Fan, H. 2014 Salinity improves chilling resistance in *Suaeda salsa*. *Acta Physiologiae Plantarum* **36** (7), 1823–1830.

Dong, L. Y., Jin, Y., Song, T., Liang, J. S., Bai, X., Yu, S. M., Teng, C. Y., Wang, X., Qu, J. J. & Wang, H. M. 2017 Removal of Cr(VI) by surfactant modified *Auricularia auricula* spent substrate: biosorption condition and mechanism. *Environmental Science and Pollution Research* **24**, 17626–17641.

Freundlich, H. & Helle, W. J. 1939 Ubber die adsorption in Lusungen. *Journal of the American Chemical Society* **61**, 2–28.

Gómez-Brandón, M., Lazcano, C. & Domínguez, J. 2008 The evaluation of stability and maturity during the composting of cattle manure. *Chemosphere* **70**, 436–444.

Harja, M., Buema, G., Sutiman, D. M., Munteanu, C. & Bucur, D. 2012 Low cost adsorbents obtained from ash for copper removal. *Korean Journal of Chemical Engineering* **29** (12), 1735–1744.

Hu, X. J., Wang, J. S., Liu, Y. G., Li, X., Zeng, G.-m., Bao, Z.-l., Zeng, X.-x., Chen, A.-c. & Long, F. 2011 Adsorption of chromium (VI) by ethylenediamine-modified cross-linked magnetic chitosan resin: isotherms, kinetics and thermodynamics. *Journal of Hazardous Materials* **185** (1), 306–314.

Hu, X. J., Yan, L. L., Gu, H. D., Zang, T. T., Jin, Y. & Qu, J. J. 2014 Biosorption mechanism of Zn^{2+} from aqueous solution by spent substrates of *Pleurotus ostreatus*. *Korean Journal of Chemical Engineering* **31**, 1911–1918.

Huang, Y., Ma, X., Liang, G. & Wang, S. 2008 Adsorption behavior of Cr(VI) on organic-modified rectorite. *Chemical Engineering Journal* **138**, 187–193.

Kalinke, C., Mangrich, A. S., Marcolino Jr, L. H. & Bergamini, M. F. 2016 Biochar prepared from castor oil cake at different temperatures: a voltammetric study applied for Pb^{2+}, Cd^{2+} and Cu^{2+} ions preconcentration. *Journal of Hazardous Materials* **318**, 526–532.

Downloaded from http://iwa.silverchair.com/wst/article-pdf/79/8/1511/617908/wst079081511.pdf
by guest

Kumar, P. A. & Chakraborty, S. 2009 Fixed-bed column study for hexavalent chromium removal and recovery by short-chain polyaniline synthesized on jute fiber. *Journal of Hazardous Materials* **162**, 1086–1098.

Kumar, R., Bhatia, D., Singh, R., Rani, S. & Bishnoi, N. R. 2011 Sorption of heavy metals from electroplating effluent using immobilized biomass *Trichoderma viride* in a continuous packed-bed column. *International Biodeterioration & Biodegradation* **65**, 1133–1139.

Kumar, S., Masto, R. E., Ram, L. C., Sarkar, P., George, J. & Selvi, V. A. 2013 Biochar preparation from *Parthenium hysterophorus* and its potential use in soil application. *Ecological Engineering* **55**, 67–72.

Kwon, T. N. & Jeon, C. 2012 Selective adsorption for indium(III) from industrial wastewater using chemically modified sawdust. *Korean Journal of Chemical Engineering* **29** (12), 1730–1734.

Lakshminarayanan, P. V., Toghiani, H. & Pittman, J. C. U. 2004 Nitric acid oxidation of vapor grown carbon nanofibers. *Carbon* **42**, 2433–2442.

Langmuir, I. 1918 The adsorption of gases on plane surface of glass, mica, and platinum. *Journal of the American Chemical Society* **40**, 1361–1403.

Lee, S. M., Laldawngliana, C. & Tiwari, D. 2012 Iron Oxide nano-particles-immobilized-sand material in treatment of Cu(II), Cd(II) and Pb(II) contaminated waste waters. *Chemical Engineering Journal* **195–196**, 103–111.

Li, F. T., Yang, H., Zhao, Y. & Xu, R. 2007 Novel modified pectin for heavy metal adsorption. *Chinese Chemical Letters* **18**, 325–328.

Liang, B., Lehmann, J., Solomon, D., Kinyangi, J., Grossman, J., O'Neill, B., Skjemstad, J. O., Thies, J., Luizão, F. J., Petersen, J. & Neves, E. G. 2006 Black carbon increases cation exchange capacity in soils. *Soil Science Society of America Journal* **70** (5), 1719–1730.

Lin, B. L., Xiu, Z. M., Liu, N., Bi, H. T. & Lv, C. X. 2012 Adsorption of lead and cadmium ions from aqueous solutions by modified oil shale ash. *Oil Shale* **29**, 268–278.

Lodeiro, P., Herrero, R. & Sastre de Vicente, M. E. 2006 The use of protonated *Sargassum muticum* as biosorbent for cadmium removal in a fixed-bed column. *Journal of Hazardous Materials* **137**, 244–253.

Luo, X. G., Liu, F., Deng, Z. F. & Lin, X. 2011 Removal of copper(II) from aqueous solution in fixed-bed column by carboxylic acid functionalized deacetylated konjac glucomannan. *Carbohydrate Polymers* **286**, 753–759.

Mattuschka, B. & Straube, G. 1993 Biosorption of metals by a waste biomass. *Journal of Chemical Technology and Biotechnology* **58**, 57–63.

Mukherjee, A., Zimmerman, A. R. & Harris, W. 2011 Surface chemistry variations among a series of laboratory-produced biochars. *Geoderma* **163**, 247–255.

Naja, G. & Volesky, B. 2006 Behavior of the mass transfer zone in a biosorption column. *Environmental Science & Technology* **40**, 3996–4003.

Njoku, V. O., Ayuk, A. A., Oguzie, E. E. & Ejike, E. N. 2012 Biosorption of Cd(II) from aqueous solution by cocoa pod husk biomass: equilibrium, kinetic, and thermodynamic studies. *Separation and Purification Technology* **47** (5), 753–761.

Nomanbhay, S. M. & Palanisamy, K. 2004 Removal of heavy metals from industrial wastewater using chitosan coated oil palm shell charcoal. *Electronic Journal of Biotechnology* **8**, 43–53.

Oguz, E. 2005 Adsorption characteristics and the kinetics of the Cr(VI) on the *Thuja oriantalis*. *Colloids and Surfaces* **252**, 121–128.

Panda, G. C., Das, S. K., Bandopadhyay, T. S. & Guha, A. K. 2007 Adsorption of nickel on husk of *Lathyrus sativus*: behavior and binding mechanism. *Colloids and Surfaces B-Biointerfaces* **57**, 135–142.

Park, J. H., Yong, S. O., Kim, S. H., Kang, S. W., Cho, J. S., Heo, J. S., Delaune, R. D. & Seo, D. C. 2015 Characteristics of biochars derived from fruit tree pruning wastes and their effects on lead adsorption. *Applied Biological Chemistry* **58** (5), 751–760.

Pels, J. R., Kapteijn, F., Moulijn, J. A., Zhu, Q. & Thomas, K. M. 1995 Evolution of nitrogen functionalities in carbonaceous materials during pyrolysis. *Carbon* **33**, 1641.

Regmi, P., Moscoso, J. L. G., Kumar, S., Cao, X., Mao, J. & Schafran, G. 2012 Removal of copper and cadmium from aqueous solution using switchgrass biochar produced via hydrothermal carbonization process. *Journal of Environmental Management* **109**, 61–69.

Rumapar, K. F., Rumhayati, B. & Tjahjanto, R. T. 2013 Adsorption of lead and copper using water hyacinth compost (*Eichhornia crassipes*). *Journal of Pure & Applied Chemistry Research* **3** (1), 27–34.

Safari, M., Sorooshzadeh, A., Asgharzadeh, A. & Saadat, S. 2013 The application of adsorption modeling and Fourier transform infrared spectroscopy to the comparison of two species of plant growth–promoting rhizobacteria as biosorbents of cadmium in different pH solutions. *Bioremediation Journal* **17** (4), 201–211.

Sari, A. & Tuzen, M. 2008 Biosorption of cadmium (II) from aqueous solution by red algae (*Ceramium virgatum*): equilibrium, kinetic and thermodynamic studies. *Journal of Hazardous Materials* **157**, 448–454.

Sheng, P. X., Ting, Y. P., Chen, J. P. & Hong, L. 2004 Sorption of lead, copper, cadmium, zinc, and nickel by marine algal biomass: characterization of biosorptive capacity and investigation of mechanisms. *Journal of Colloid and Interface Science* **275**, 131–141.

Song, T., Yu, S. M., Wang, X., Teng, C., Bai, X., Liang, J., Dong, L., Ouyang, F., Qu, J. & Jin, Y. 2017a Biosorption of lead(II) from aqueous solution by sodium hydroxide modified *Auricularia auricular* spent substrate: isotherms, kinetics, and mechanisms. *Water Air and Soil Pollution* **228**, 236.

Song, T., Liang, J. S., Bai, X., Teng, C., Bai, X., Liang, J., Dong, L., Ouyang, F., Qu, J. & Jin, Y. 2017b Biosorption of cadmium ions from aqueous solution by modified *Auricularia auricular* matrix waste. *Journal of Molecular Liquids* **241**, 1023–1031.

Tan, G. Q. & Xiao, D. 2009 Adsorption of cadmium ion from aqueous solution by ground wheat stems. *Journal of Hazardous Materials* **164**, 1359–1363.

Downloaded from http://iwa.silverchair.com/wst/article-pdf/79/8/1511/617908/wst079081511.pdf
by guest

Tee, T. W. & Khan, A. R. M. 1988 Removal of lead, cadmium and zinc by waste tea leaves. *Environmental Science & Technology Letters* **9**, 1223–1232.

Torab-Mostaedi, M., Asadollahzadeh, M., Hemmati, A. & Khosravi, A. 2013 Equilibrium, kinetic, and thermodynamic studies for biosorption of cadmium and nickel on grapefruit peel. *Journal of the Taiwan Institute of Chemical Engineers* **44**, 295–302.

Tuzun, I., Bayramoglu, G., Alcin, Y. E., Başaran, G., Celik, G. & Arica, M. Y. 2005 Equilibrium and kinetic studies on biosorption of Hg(II), Cd(II) and Pb(II) ions onto microalgae Chlamydomonas reinhardtii. *Journal of Environmental Planning and Management* **77**, 85–92.

Vimala, R. & Das, N. 2009 Biosorption of cadmium (II) and lead (II) from aqueous solutions using mushrooms: a comparative study. *Journal of Hazardous Materials* **168**, 376–382.

Wahab, M. A., Jellali, S. & Jedidi, N. 2010 Ammonium biosorption onto sawdust: FTIR analysis, kinetics and adsorption isotherms modeling. *Bioresource Technology* **101** (14), 5070.

Wang, X., Cook, R., Tao, S. & Xing, B. 2007 Sorption of organic contaminants by biopolymers: role of polarity, structure and domain spatial arrangement. *Chemosphere* **66**, 1476.

Zhou, J. H., Sui, Z. J., Zhu, J., Li, P., Chen, D., Dai, Y. C. & Yuan, W. K. 2007 Characterization of surface oxygen complexes on carbon nanofibers by TPD, XPS, and FT-IR. *Carbon* **45**, 785–796.

First received 11 October 2018; accepted in revised form 16 April 2019. Available online 23 April 2019

Downloaded from http://iwa.silverchair.com/wst/article-pdf/79/8/1511/617908/wst079081511.pdf
by guest